Modeling of Rate-based Congestion Control Schemes in Cognitive Radio Sensor Networks

Vahid Esmaeelzadeh[a], Elahe S. Hosseini[a], Reza Berangi[a], Ozgur B. Akan[b]

[a] *Wireless Networks Laboratory (WNL), Department of Computer Engineering, Iran University of Science and Technology, Tehran, Iran.*
[b] *Next-generation and Wireless Communications Laboratory (NWCL), Department of Electrical and Electronics Engineering, Koc University, Istanbul, Turkey*

Abstract

Performance evaluation of transport layer protocols in cognitive radio sensor networks (CRSNs) is useful to provide quality-of-service for real-time reliable applications. This paper develops an analytical framework to model the steady-state sending rate of collecting cognitive radio (CR) sensors in rate-based generic additive-increase multiplicative-decrease (AIMD) and additive-increase additive-decrease (AIAD) congestion control schemes. Evolution process of sending rate is modeled by a discrete time Markov chain (DTMC) in the terms of queue length. We model the queue length distribution of a CR node by a semi-Markov chain (SMC) with assuming general probability density functions (PDFs) of input rate and attainable sending rate of the node. These PDFs are derived based on the parameters of MAC and physical layers and CRSN configuration. The proposed models are verified through various simulations.

Keywords: Cognitive radio sensor networks, rate-based congestion control, steady-state rate distribution

1. Introduction

Cognitive radio technology is highly used as a capable tool to alleviate the spectrum underutilization problem and provide dynamic spectrum access (DSA) in wireless networks [1]. In this way, a CR-equipped node uses unlicensed spectrum bands opportunistically based on CR basic operations: spectrum sensing, decision and handoff [2]. Licensed users in cognitive radio networks are called primary users (PUs) which have priority to access the licensed bands [1]. CR users can use the licensed bands in the absence of PUs. If a primary user is appeared in the licensed band, CR user leaves the spectrum immediately [1]. Cognitive radio technology can be used in wireless sensor networks (WSNs) to

Email addresses: v_esmaeelzadeh@iust.ac.ir (Vahid Esmaeelzadeh), elahe_hosseini@iust.ac.ir (Elahe S. Hosseini), rberangi@iust.ac.ir (Reza Berangi), akan@ku.edu.tr (Ozgur B. Akan)

overcome spectrum shortage problem and reserve the limited resources of sensors in WSNs [3]. Wireless sensor networks with CR-equipped sensor nodes are called cognitive radio sensor networks (CRSNs) [3]. With regard to the application, opportunistic spectrum access (OSA) feature of sensor nodes in CRSNs can decrease the collision and retransmission probabilities in the environments with bursty traffic which is common in sensor networks. Moreover, adaptive spectrum access of CR sensors in dynamic wireless channels increases the transmission efficiency which leads to less power consumption [3].

Primary users' activities and unique features of CRSNs such as spectrum sensing and spectrum mobility affect the performance of MAC, routing and transport layer protocols. Disregarding these effects may lead to the violation of main objectives of CRSNs. Hence, the performance evaluation of the protocols of MAC, network and transport layers with regard to CR-related parameters is crucial for CRSNs. In this paper, we focus on the performance evaluation of transport layer in CRSNs.

The performance of transport layer protocols is important in the QoS of various applications in CRSNs. However, there is a limited amount of work on the performance evaluation of transport layer protocols in CRSNs. Most of previous studies [4, 5, 6, 7, 8, 9, 10, 11, 12, 13, 14] concentrated on the simulation-based performance evaluation of transport layer protocols. However, analytical investigation is required to model the performance of congestion control schemes in CRSNs for the following motivations: (1) Transport-level delay (delay overhead of transport layer protocols) depends on the sending rate of source nodes in this layer. Sending rate of collecting CR sensors is controlled through the rate-based congestion control schemes by considering the congestion status of CR nodes in the network. (2) In real-time reliable applications, it is necessary to consider delay and reliability. Modeling the transport layer sending rate and congestion probability in CRSNs helps to investigate analytically real-timeness and reliability which makes better QoS provisioning in different applications. To the best of our knowledge, there is no analytical framework to calculate the sending rate distribution of CR source sensors based on the queue length distribution and MAC delay overhead of CR nodes in the current literature.

In this paper, an analysis of rate-based generic AIMD and AIAD congestion control schemes in CRSNs is presented. The main contributions are the following:

- An analytical model is proposed for the sending rate distribution of collecting CR sensors. The simulation experiments verify the sending rate model.
- In order to model the distribution of sending rate in the transport layer of collecting CR sensors, a stochastic congestion model is proposed. In this way, the queue length of CR nodes is assumed to be the congestion detection parameter. The queue length distribution of a CR node depends on the distribution of input rate and attainable sending rate of the node. Usually, the queue length distribution of a node is modeled by assuming that arrivals follow a Poisson process and the service time of a node has an

exponential distribution. However, these assumptions are not always applicable. We do not make any assumption about the input and attainable sending rate distribution of CR nodes. Therefore, a semi-Markov chain (SMC) is proposed to model the queue length distribution of different nodes in CRSN.

- In order to accomplish the SMC, the probability density functions (PDFs) of input and attainable sending rates of different CR nodes are derived. These PDFs are calculated based on the proposed models of CR attainable sending rate on the channel, the delay overhead of MAC-layer and the CRSN configuration.

The rest of this paper is organized as follows. Section 2 reviews the related work addressing the performance evaluation of transport layer protocols in CRSNs and CRNs. Also, this section describes the congestion control schemes in WSNs. In Section 3, system model of the CRSN is defined. Section 4 models the sending rate distribution of a collecting CR sensor in the CRSN. Stochastic model of congestion in the CRSN is explained in Section 5. Analytical results and verifications are presented in Section 6. Finally, in Section 7, conclusions are presented.

2. Related Work

In this section, we review the current research studies in the literature addressing the performance evaluation of transport layer protocols in CRNs and CRSNs. Furthermore, we review the congestion control schemes and explain the main modules of transport layer in WSNs.

2.1. Performance evaluation of transport layer protocols in CRSNs and CRNs

In [4], the performance of existing congestion control schemes is studied over cognitive radio sensor networks to reveal the CRSN challenges for transport layer protocols. Authors in [5] investigate the challenges of real-time transport over CRSNs in the different spectrum environments of smart grid. In [15], the optimality of simple rate adjustment techniques is investigated in CRSNs. In [16], the stochastic backlog and delay bounds of generic AIMD congestion control schemes in CRSNs are modeled based on stochastic network calculus (SNC) [17]. The [16] models the backlog and delay bounds with the given sending rate distribution (probability mass function) of source nodes in CRSNs through moment generating function (MGF)-based theories in SNC. However, there is no modeling of sending rate distribution of CR source sensors based on queue length distribution and the attainable sending rate of MAC layer in CRSNs that is the main contribution of this study.

Although CRSN is a new research area to be studied for performance evaluation of transport layer protocols, there is a significant amount of research on evaluating the performance of TCP over cognitive radio networks (CRNs). In

[6], TCP efficiency and throughput over CRNs are studied. The impact of primary users' traffic, the number of wireless channels and sensing period on the throughput of TCP is investigated in [7]. In [8], the behavior of TCP throughput, round trip time (RTT) and congestion window size are studied based on sensing frequency, primary users' traffic and the heterogeneity of channels. In [9], a transport protocol for cognitive radio ad-hoc networks is proposed. Furthermore, the impact of sensing time on TCP throughput is considered. Also, the effect of alternations in the available bandwidth of CR users on the behavior of TCP congestion control is studied. Authors in [10] discuss the TCP performance degradation in CRNs through considering the congestion window size, RTT behavior and retransmission timeout (RTO). In [12], TCP throughput is evaluated based on primary users' activities and the number of available wireless channels. An equation-based transport protocol for cognitive radio networks is proposed in [13]. Authors in [14] evaluate TCP end-to-end delay, throughput and packet drop probability with regard to packet size, sensing time, sensing accuracy and activities of primary users. However, most of studies have focused on the simulation-based performance evaluation of transport layer protocols in CRNs.

2.2. Congestion Control Schemes

In the literature, different transport layer protocols have been proposed for WSNs. The papers [18, 19] comprehensively review the transport layer and congestion control schemes in WSNs. Studying the transport layer protocols in sensor networks can help us to define and extract a basic core of congestion control schemes which is comprised of the simple rate adjustment algorithms as the congestion avoidance techniques and the buffer occupancy of network nodes as the congestion detection metric.

Generally, a transport protocol in WSNs can have three main modules: (1) congestion module, (2) reliability module and (3) priority module [18]. The submodules of congestion module are congestion detection, congestion notification and congestion avoidance. The congestion detection is the identification of some events which may cause congestion in the network. The protocols ESRT [20], RT^2 [21], CODA [22], Fusion [23], Siphon [24], STCP [25], DST [26] and CTCP [27] use the buffer occupancy as the congestion detection metric. The protocol TRCCIT [28] uses the packet rate for congestion detection. The node delay is used as the congestion detection metric in [21, 26]. The papers [29, 30] consider the packet inter-arrival time and packet service time in order to predict the congestion in the network. Some other metrics such as channel status [22] and reliability parameters [31, 32] are used to detect congestion in WSNs.

Two common congestion avoidance techniques which are used in various congestion control schemes are: rate adjustment and traffic redirection. There are two types of rate adjustment algorithms: simple rate adjustment and exact rate adjustment [18]. The protocols STCP [25], Flush [33], CODA [22], ESRT [20], RCRT [31] use simple rate adjustment techniques such as additive increase multiplicative decrease (AIMD) and additive increase additive decrease (AIAD). The exact rate adjustment technique is considered in [28, 21, 26, 29, 34]. The traffic redirection technique is used in some protocols such as PORT [32], STCP [25] and Siphon [24].

In this paper, based on the main modules of transport layer in WSNs, we model the basic rate-based congestion control schemes which can be used as an analytical framework for the modeling of various rate-based congestion control schemes in WSNs and CRSNs. The buffer occupancy (queue length) is considered as congestion detection metric. The simple AIMD and AIAD rate adjustment techniques are used as congestion avoidance techniques.

3. System Model

Partitioning low quality wireless links with long distances into several high quality short distance links (via relay nodes) is introduced to enable the event delivery between the sensor nodes and the sink station. Using multi-hop relay nodes can decrease the path loss probability and increase the lifetime of resource-limited sensors in WSNs [35]. In this article, a CRSN with some collecting CR sensors and multi-hop CR relay nodes are considered. The CR relay nodes forward the received data from the collecting CR sensors toward the sink station. The network model is illustrated in Fig. 1. The network consists of three types of nodes: collecting CR sensors, CR relay nodes and sink station. The CR relay nodes are grouped in different groups based on the distance to the sink and collecting sensors.

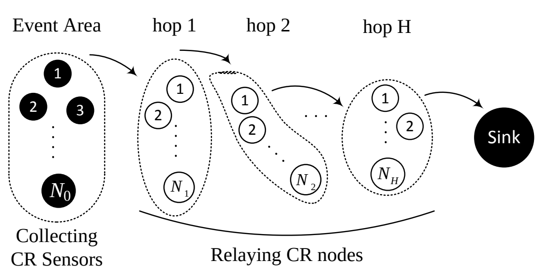

Figure 1: CRSN topology. Collecting CR sensors send data via CR relay nodes toward the sink station. Data transfer at each hop is affected by the activity of primary users in the licensed spectrum channels.

Relay nodes are grouped in H hops and the relays in group h are named h-hop relays ($1 \leq h \leq H$). The group of h-hop relays is assumed to consist of N_h relay nodes. Nodes are indexed with (h,n_h) where h and n_h are hop index and node index in h-hop relays, respectively ($1 \leq n_h \leq N_h$). There are N_0 collecting CR sensors in the event area. In other words, the 0-hop nodes are equivalent to CR collecting sensors ($1 \leq n_0 \leq N_0$).

A CR node has two main modes: sensing mode and operating mode. First, a CR node senses the licensed spectrum to decide whether it is idle or occupied by a primary user (PU). Sensing time and sensing frequency are denoted by t_s and f_s, respectively. It is also assumed that the sensing is done ideally and there is no sensing error. After sensing, the CR node enters in the operating mode and send data in a licensed spectrum channel if it is free of PUs.

Primary users' activity is modeled as exponentially distributed interarrivals. The traffic of a primary user can be modeled as a two-state entrance-departure process with the entrance rate of β and the departure rate of α [36]. A primary user has two states: ON and OFF. The ON state represents the period that primary user operates in a channel and the CR node cannot use the channel. The OFF state represents the period that the primary user does not operate in a channel and the CR nodes can use the channel. There are N_{ch} wireless channels with the same bandwidth. In each channel, a PU operates based on its entrance rate (β) and departure rate (α). When a PU starts to operate on its licensed channel, the operations of each active CR node on the licensed channel in the CRSN will be stopped.

We focus on a basic transport protocol which supports only congestion control. In this paper, the queue length (buffer occupancy level) of nodes is assumed to be the metric for the detection of congestion in the network. Congestion avoidance is usually done through rate adjustment techniques. The regulating of the sending rate of collecting sensors with regard to the reception of congestion notification is called rate adjustment. Rate adjustment algorithms can be categorized into two main classes [18]: simple rate adjustment and exact rate adjustment. In simple rate adjustment algorithms, the rate controlling operation is done based on a single congestion bit such as additive increase multiplicative decrease (AIMD). In the exact rate adjustment algorithms, the rate adjusting operation is performed based on the notified congestion degree. In this paper, we consider the generic AIMD and AIAD rate adjustments as the congestion avoidance mechanisms which are realized centrally in the sink station. The control decisions are made by the sink station and sent to the collecting CR sensors. The minimum value of the sending rate is assumed to be 1 packet per second. We also assume that there is a sink buffer limitation on the collecting CR sensors' sending rate with the maximum rate value of R_{max} packets per second. The queue size of collecting sensors and relays is given by B and the queue length threshold for the detection of congestion is denoted by l_{max}.

4. Sending rate distribution of a collecting CR sensor in CRSNs

Sending rate distribution of collecting sensors is calculated under the following basic assumptions:

- The minimum value of sending rate is 1 packet per second.
- There is a sink buffer limitation on the CR sensor nodes' sending rate with the maximum rate value of R_{max} packets per second.
- All nodes inform their congestion status to the sink. The congestion avoidance scheme is run centrally by the sink station and the congestion-related

notification commands are sent from the sink to the collecting sensor nodes at each congestion notification period T.

- All congestion notification packets are communicated through common control channel [37] so that there is no packet loss in the communication of the congestion notification packets.
- The congestion avoidance is realized based on rate-based generic AIMD and AIAD schemes with INC and DEC as rate increasing and rate decreasing factors, respectively [38].

For a rate-based generic AIMD scheme, the sending rate evolution process is as follows:

$$r_{i+1} = \begin{cases} \max(1, \lfloor \frac{r_i}{\mathrm{DEC}} \rfloor) & \text{with probability } \Omega_{r_i} \\ \min(r_i + \mathrm{INC}, R_{max}) & \text{with probability } 1 - \Omega_{r_i} \end{cases} \tag{1}$$

and also for the rate-based generic AIAD scheme

$$r_{i+1} = \begin{cases} \max(1, r_i - \mathrm{DEC}) & \text{with probability } \Omega_{r_i} \\ \min(r_i + \mathrm{INC}, R_{max}) & \text{with probability } 1 - \Omega_{r_i} \end{cases} \tag{2}$$

where r_i is the current sending rate of a collecting sensor node and Ω_{r_i} is the congestion probability in the established path between the source node (collecting CR sensor) and the sink while sending rate of source node is r_i. The r_{i+1} is the new adjusted sending rate of the source node. The rate-based generic AIMD and AIAD schemes increase the sending rate additively by INC factor if there is no congested node at the path from the source node to the sink in the congestion notification period, i.e., T. The AIMD/AIAD scheme decreases the sending rate multiplicatively/additively by DEC if a congestion is detected at the path from the source node to the sink node in the period of T. Congestion-related notifications are decided by the sink station periodically with the period of T. Congestion notification packets are communicated through common control channel [37]. Therefore, it is reasonable to assume that there is no packet loss in the communication of notification packets. Furthermore, the notification packets are forwarded in different nodes with high priority so that the communication delay of congestion notification is so smaller than the congestion notification period, i.e., T. Hence, the communication delay of the congestion notification is negligible in comparison to T.

In Fig. 2, the semi Markov chain (SMC) representing the evolution process of the sending rate of a collecting CR sensor based on generic AIMD rate adjustment is illustrated for maximum sending rate $R_{max} = 8$, increasing factor INC=1 and decreasing factor DEC=2. The sending rate evolution process $\{r_i\}$ is an irreducible, finite state, aperiodic Markov chain; hence the embedded DTMC of SMC has a unique steady state distribution [39]. Calculating the steady state distribution of embedded DTMC, i.e., $\pi = (\pi_1, \pi_2, \ldots, \pi_{R_{max}})$, can be done by solving a system of linear equations with R_{max} independent equations and R_{max} unknown variables. Since the sojourn time of all states almost equals to T (because the congestion notification delay is so smaller than T), the steady state distribution of SMC equals to the steady state distribution of its embedded DTMC, because:

$$P_r = \frac{\pi_r T}{\sum_{r=1}^{R_{max}} \pi_r T} = \frac{\pi_r T}{T} = \pi_r \qquad r = 1, 2, ..., R_{max} \tag{3}$$

where the $(P_1, P_2, \ldots, P_{R_{max}})$ is the steady state distribution of the SMC and the $(\pi_1, \pi_2, \ldots, \pi_{R_{max}})$ is the steady state distribution of the embedded DTMC.

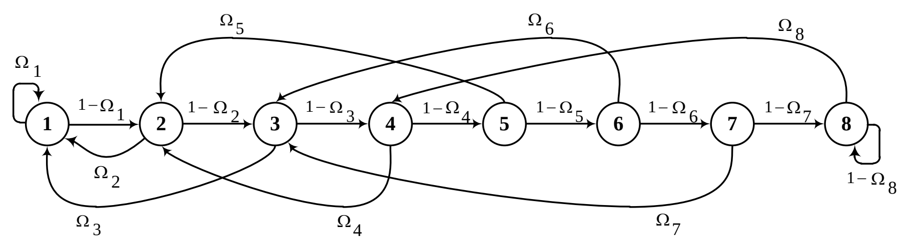

Figure 2: The semi Markov Chain representing the evolution process of a collecting CR sensor sending rate based on generic AIMD rate adjustment with maximum sending rate $R_{max} = 8$, the increasing factor INC=1 and the decreasing factor DEC=2. The Ω_{r_i} $(r_i = 1, 2, ..., R_{max})$ is the congestion probability in the path between the source node and sink while the sending rate of source node is r_i.

The steady state distribution of the sending rate of source nodes depends on the congestion probabilities of the nodes in the path between the source node and the sink, i.e., $\Omega_1, \Omega_2, ..., \Omega_{R_{max}}$. In the next section, the congestion probabilities of CR nodes are calculated in CRSNs.

5. Stochastic model of congestion in CRSNs

The queue length is considered as the congestion detection parameter. Therefore, in order to calculate the congestion probabilities, we need to model the queue length distribution of a CR node in CRSNs.

5.1. Queue length distribution of a CR node in CRSNs

The steady state distribution of a node queue length is modeled usually by assuming that arrivals follow a Poisson process and the service time of the node has an exponential distribution. Note that, these assumptions are not always applicable. We model the queue length distribution by deriving the probability density functions (PDFs) of the input rate and the attainable sending rate of a CR node. In other words, we do not consider any assumption about the input and attainable sending rate distribution of CR nodes.

Since the future behavior of the queue length is completely characterized by its current state, the underlying stochastic model will be a semi-Markov chain (SMC) [39]. To completely specify the SMC of queue length, the density functions of the input rate and the attainable sending rate of a CR node are required. An SMC is a generalization of a continuous-time Markov chain (CTMC) in which the time between transitions from one state to another is not exponentially distributed but rather is generally distributed [39]. If the behavior of an SMC is observed at discrete instances that the state transitions occur, its embedded DTMC will be obtained.

Let **RI** and **RS** be two continuous random variables representing the input rate and attainable sending rate of a CR node. The queue length increases with the probability of $P(\mathbf{RI}{>}\mathbf{RS})$ and decreases with the probability of $P(\mathbf{RI}{<}\mathbf{RS})$ where $P(\mathbf{RI}{>}\mathbf{RS})$ is the probability that the input rate is greater than the attainable sending rate and $P(\mathbf{RI}{<}\mathbf{RS})$ is the probability that the input rate is less than the attainable sending rate. The embedded DTMC of queue length is depicted in Fig. 3 where each state represents the queue length and B denotes the queue size of the node.

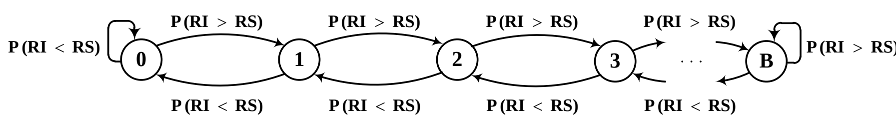

Figure 3: The embedded DTMC of queue length for a CR node with the queue size of B. Each state represents the queue length. The **RI** and **RS** are continuous random variables representing the input rate and the attainable sending rate of the CR node, respectively.

Transition probabilities. Since **RI** and **RS** are continuous random variables, we have $P(\mathbf{RI} = \mathbf{RS}) = 0$; as a result, we will obtain

$$P(\mathbf{RI} > \mathbf{RS}) + P(\mathbf{RI} < \mathbf{RS}) = 1. \tag{4}$$

According to the total probability theorem [39], we have

$$P(\mathbf{RI} < \mathbf{RS}) = \int_{-\infty}^{\infty} P(\mathbf{RI} < \mathbf{RS} | \mathbf{RS} = r) f_{\mathbf{RS}}(r) dr \tag{5}$$

where $f_{\mathbf{RS}}(r)$ is the probability density function of **RS**. Steady state distribution of node queue length is calculated based on the transition probabilities of the embedded DTMC as follows:

$$Q_l = \frac{\left(1 - \frac{P(\mathbf{RI}>\mathbf{RS})}{P(\mathbf{RI}<\mathbf{RS})}\right)\left(\frac{P(\mathbf{RI}>\mathbf{RS})}{P(\mathbf{RI}<\mathbf{RS})}\right)^l}{1 - \left(\frac{P(\mathbf{RI}>\mathbf{RS})}{P(\mathbf{RI}<\mathbf{RS})}\right)^{B+1}} \quad l = 0, 1, ..., B \tag{6}$$

where l is node queue length and Q_l is the probability that the queue length equals l. To calculate the queue length distribution of a node in the CRSN, it is needed to calculate the PDFs of input rate of the node, i.e., $f_{\mathbf{RI}}(r)$ and the attainable sending rate of the node, i.e., $f_{\mathbf{RS}}(r)$.

5.2. Probability density function of the attainable sending rate of a CR node

In the operating mode, a CR node operates based on a multichannel MAC protocol of which its behavior is inspired from the CSMA/CA mechanism [14].

The CR node first senses the spectrum and selects a channel which is free of primary users. After selecting a free channel, CR node enters into the operating mode to send data on the selected channel. In the operating mode, if CR node has a packet to send, it selects a random double backoff time BT from the range $[0, BT_{min}]$ with a continuous uniform distribution, where BT_{min} is the minimum backoff time. At the end of the first backoff period, the carrier sensing is realized on the considered channel; if the channel is free of the other CR nodes, the sending of packet is started; else an exponential backoff algorithm is started again. The backoff algorithm is performed continuously. CR nodes are only permitted to commence their transmissions at the end of the backoff time. In the backoff attempt i, BT is randomly selected from the range $[0, 2^i BT_{min}]$ with a continuous uniform distribution. Backoff attempts are repeated until the channel is free of CR nodes at the end of the backoff period, or until the maximum number of backoff attempts (K) is reached; after that the packet is sent. At the end of the operating mode, CR node operations are stopped and the node enters into the spectrum sensing mode again. If the node cannot find a free channel in the spectrum sensing period, enters into the operating mode without sending any packet. In the next sensing period, the node has another chance to find a free channel; if there is no free channel for second time, the packet will be dropped. The handoff time between two channels by a CR user will increase the MAC delay overhead slightly. In our modeling, the handoff time is ignored.

Let $\mathbf{D}_{op}$ be a continuous random variable representing the MAC delay overhead of a CR node in its operating mode. We have

$$\mathbf{D}_{op} = \sum_{i=0}^{K-1} p_b^i \mathbf{BT}_i \tag{7}$$

where $\mathbf{BT}_i$ is a random variable with continuous uniform distribution, i.e., $\mathbf{BT}_i \sim U(0, 2^i BT_{min})$; the backoff probability is denoted by p_b which is the probability that all channels are sensed busy in the carrier sensing. In Section 5.4, the backoff probability will be calculated.

The probability density functions of $\mathbf{BT}_i$ are as follows:

$$f_{\mathbf{BT}_i}(t) = \begin{cases} \frac{1}{2^i BT_{min}} & 0 \le t \le 2^i BT_{min} \\ 0 & \text{otherwise.} \end{cases} \tag{8}$$

The probability density function of $p_b^i \mathbf{BT}_i$ is calculated as follows [40]:

$$f_{p_b^i \mathbf{BT}_i}(t) = \begin{cases} \frac{1}{p_b^i 2^i BT_{min}} & 0 \le t \le p_b^i 2^i BT_{min} \\ 0 & \text{otherwise.} \end{cases} \tag{9}$$

Consequently, the probability density function of the random variable $\mathbf{D}_{op}$ is obtained as follows [40]:

$$f_{\mathbf{D}_{op}}(t) = f_{\mathbf{BT}_0}(t) * f_{p_b\mathbf{BT}_1}(t) * f_{p_b^2\mathbf{BT}_2}(t) ... * f_{p_b^{K-1}\mathbf{BT}_{K-1}}(t). \tag{10}$$

Sensing efficiency (ω) is the ratio of operating time over the sum of the sensing time and the operating time as follows [36]:

$$\omega = \frac{t_o}{t_s + t_o} = 1 - t_s f_s \tag{11}$$

where t_o is the operating time of a CR node and the f_s (the frequency of performing spectrum sensing by a CR node) equals to $\frac{1}{t_s+t_o}$.

The probability of the channel being busy by PU is [36]

$$P_{on} = \frac{\beta}{\alpha + \beta} \tag{12}$$

where α and β are the departure and entrance rates of PU in a channel, respectively. The probability that at least one channel is free of the PU is

$$P_{off} = 1 - (P_{on})^{N_{ch}} \tag{13}$$

where N_{ch} is the number of channels.

For the attainable sending rate of a CR node, i.e., $\mathbf{RS}$, we have

$$\mathbf{RS} = \frac{1}{\mathbf{D}} \tag{14}$$

where $\mathbf{D}$ is the continuous random variable representing the MAC delay overhead of a CR node. The $\mathbf{D}$ is calculated as follows:

$$\mathbf{D} = \omega \left(P_{off}(\mathbf{D}_{op} + \frac{8 \times S_{pkt}}{C}) + (1 - P_{off})\mathbf{D}_{pu} \right) + (1 - \omega)\mathbf{D}_s \tag{15}$$

where $(1 - \omega)$ is the probability of being in the sensing mode. When a packet is received in MAC layer in order to send over the channel, the node is either in the operating mode with the probability of ω or in the sensing mode with the probability of $1 - \omega$. The $\mathbf{D}_s$ is the delay overhead of being in sensing mode for each packet. At operating mode, the node has a free channel of PUs in order to send the packet with the probability of P_{off} and does not have a free channel of PUs with the probability of $1 - P_{off}$. The $\mathbf{D}_{pu}$ is the delay overhead of not having a free channel of PUs for each packet. The C is the wireless channel capacity in bits per second and the S_{pkt} is the packet size in bytes; hence, the $\frac{8 \times S_{pkt}}{C}$ is the transmission delay of a packet over the channel.

The $\mathbf{D}_s$ is calculated as follows:

$$\mathbf{D}_s = \begin{cases} \frac{t_s - \frac{1}{2\overline{\mathbf{R}}_{in}}}{\overline{pkt}_s} + \mathbf{D}_{op} + \frac{8 \times S_{pkt}}{C} & \overline{pkt}_s \geq 1 \\ 0 & \overline{pkt}_s = 0 \end{cases} \tag{16}$$

$$\overline{pkt}_s = \min(\left\lfloor \overline{\mathbf{R}}_{in}(t_s - \frac{1}{2\overline{\mathbf{R}}_{in}}) \right\rfloor, B) \tag{17}$$

where the $\overline{\mathbf{R}}_{in}$ is the mean input rate of the MAC layer. The $t_s - \frac{1}{2\overline{\mathbf{R}}_{in}}$ is the mean remaining time of the sensing mode. The $\overline{pkt}_s$ is the mean number of packets enter into the MAC layer during the mean remaining time of sensing mode. The B is the queue size of network layer. The $\lfloor x \rfloor$ is the nearest integer value less than or equal to x.

Similarly, the $\mathbf{D}_{pu}$ is obtained as follows:

$$\mathbf{D}_{pu} = \begin{cases} \frac{t_o - \frac{1}{2\overline{\mathbf{R}}_{in}} + t_s}{\overline{pkt}_{pu}} + \mathbf{D}_{op} + \frac{8 \times S_{pkt}}{C} & \overline{pkt}_{pu} \geq 1 \\ 0 & \overline{pkt}_{pu} = 0 \end{cases} \tag{18}$$

$$\overline{pkt}_{pu} = \min(\left\lfloor \overline{\mathbf{R}}_{in}(t_o - \frac{1}{2\overline{\mathbf{R}}_{in}} + t_s) \right\rfloor, B) \tag{19}$$

where the $t_o - \frac{1}{2\overline{\mathbf{R}}_{in}}$ is the mean remaining time of operating mode. The $\overline{pkt}_{pu}$ is the mean number of packets enter into the MAC layer during the node does not have a free channel of PUs.

5.3. Probability density functions of input and output rates of CR nodes

For the node (h, n_h), the random variables of input and output rates are denoted by $\mathbf{RI}_{h,n_h}$ and $\mathbf{RO}_{h,n_h}$, respectively. The probability density functions of $\mathbf{RI}_{h,n_h}$ and $\mathbf{RO}_{h,n_h}$ are represented by $f_{\mathbf{RI}_{h,n_h}}(r)$ and $f_{\mathbf{RO}_{h,n_h}}(r)$, respectively. In this section, the probability density functions $f_{\mathbf{RI}_{h,n_h}}(r)$ and $f_{\mathbf{RO}_{h,n_h}}(r)$ are calculated for each node (h, n_h) in the CRSN.

5.3.1. PDFs of input and output rates of CR collecting sensors

According to the congestion control scheme described in Section 3, sending rate in the transport layer of the CR collecting sensors is adjusted based on the received control decisions from the sink station. Let R_{0,n_0} be the adjusted rate of CR collecting sensor n_0 in the congestion control scheme of the transport layer. Output rate of a CR collecting sensor is a random variable which depends on the attainable sending rate, i.e., $\mathbf{RS}$, and the adjusted rate of CR collecting sensors in the transport layer, i.e., R_{0,n_0}. We have for the CR collecting sensor n_0

$$\mathbf{RO}_{0,n_0} = \min(R_{0,n_0}, \mathbf{RS}) \qquad n_0 = 1, ..., N_0 \tag{20}$$

where $\mathbf{RO}_{0,n_0}$ is a random variable that represents the output rate of collecting sensor n_0 and the N_0 is the number of collecting sensors. Probability density function of $\mathbf{RO}_{0,n_0}$ is simply obtained based on the R_{0,n_0} and the PDF of $\mathbf{RS}$.

5.3.2. PDFs of input and output rates of CR relay nodes

The PDFs of input and output rates of CR relays depend on the routing protocol used and the established routes between CR collecting sensors and the sink station. A node selects one of the next hop nodes in order to forward a particular packet with a certain probability, which does not change rapidly overtime. These types of routing protocols usually are used in WSNs [35]. We consider the steady-state behavior of the routing protocol [41]. In this way, our modeling will not depend on a specific routing protocol and can be applied on any routing protocol if we have its steady-state behavior. A CR node in hop h forwards a particular packet to any of $(h+1)$-hop relays with the probability of $P^{FW}_{n_h,n_{h+1}}$ where $h = 0, ..., H$, $n_h = 1, ..., N_h$ and $n_{h+1} = 1, ..., N_{h+1}$.

The input rate of a CR relay node depends on the drop and collision probabilities of the packets which are sent from different nodes of previous hop. The collided and dropped packets are not queued in the CR relay node of next hop and the input rate of the relay node decreases based on the packet drop and collision probabilities. Therefore, the $\mathbf{RI}_{h,n_h}$ is obtained for all $h = 1, ..., H$ and $n_h = 1, ..., N_h$ as follows:

$$\mathbf{RI}_{h,n_h} = (1 - (P^{col}_{h,n_h} + P_{DRP})) \sum_{i=1}^{N_{h-1}} P^{FW}_{i,n_h} \mathbf{RO}_{h-1,i} \tag{21}$$

where P^{col}_{h,n_h} is the collision probability in the CR relay node (h, n_h) and the P_{DRP} is the packet drop probability in MAC layer. In Section 5.4, packet collision and drop probabilities will be calculated.

The $\mathbf{RO}_{h,n_h}$ is obtained for all $h = 1, ..., H$ and $n_h = 1, ..., N_h$ as follows:

$$\mathbf{RO}_{h,n_h} = \min(\mathbf{RI}_{h,n_h}, \mathbf{RS}). \tag{22}$$

5.4. Backoff, packet collision and drop probabilities

At operating phase of MAC layer, each CR node is at one of the following states: backoff states, sending state and dropping state. Let us adopt the notations BF_i, SND and DRP representing the backoff state i $(i = 0, ..., K-1)$, sending and dropping states, respectively.

Since the sojourn times of a CR node at different states of MAC layer are not exponentially distributed and the future behavior of CR node is completely characterized by its current state, we have a semi-Markov chain (SMC). If the behavior of the SMC is observed at discrete instances that the state transitions occur, we will have its embedded DTMC. The embedded DTMC of a CR node states in the MAC layer is depicted in Fig. 4. In this embedded DTMC, the transition probabilities are

$$\begin{cases} P\{\mathrm{BF}_i|\mathrm{BF}_{i+1}\} = p_b & i = 0, 1, ..., K-1 \\ P\{\mathrm{BF}_i|\mathrm{SND}\} = 1 - p_b & i = 0, 1, ..., K-1 \\ P\{\mathrm{BF}_{K-1}|\mathrm{DRP}\} = p_b & \\ P\{\mathrm{DRP}|\mathrm{BF}_0\} = 1 & \\ P\{\mathrm{SND}|\mathrm{BF}_0\} = 1. & \end{cases} \tag{23}$$

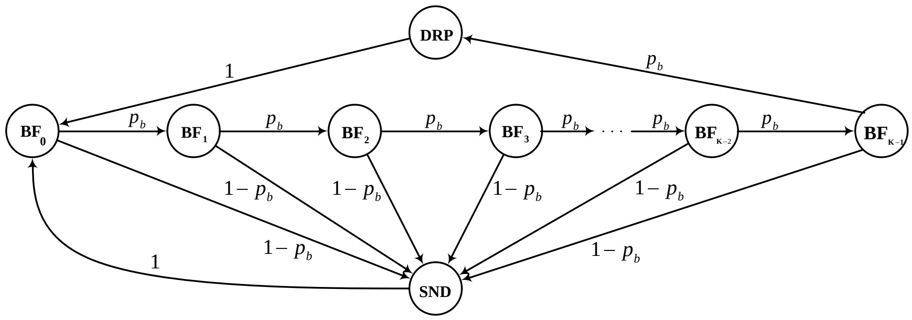

Figure 4: The embedded DTMC of a CR node states in MAC layer. The BF_i, SND and DRP states represent the backoff state i ($i = 0, ..., K-1$), sending and dropping states respectively.

First equation in Eq. 23 denotes the fact that, a CR node starts the new backoff with the backoff probability, i.e., p_b. The second equation denotes the fact that a CR node starts the sending when it is not needed to new backoff which occurs with the probability $1-p_b$. After the last backoff attempt, the CR node starts dropping the current packet if there is no free channel which occurs with the probability of p_b (the third equation). The last two equations denote the fact that a CR node starts first backoff for new packet after dropping or sending the previous packet with the probability of 1.

The steady state distribution of the embedded DTMC of Fig. 4 is

$$\begin{aligned}
\pi_{\mathrm{BF}_i} &= \frac{p_b^i}{1+\sum_{i=0}^{K-1} p_b^i} \qquad i = 0, ..., K-1 \\
\pi_{\mathrm{SND}} &= \frac{1-p_b^K}{1+\sum_{i=0}^{K-1} p_b^i} \\
\pi_{\mathrm{DRP}} &= \frac{p_b^K}{1+\sum_{i=0}^{K-1} p_b^i}
\end{aligned} \tag{24}$$

which are the probabilities that a CR node starts BF_i, SND and DRP states, respectively.

Let t_{BF_i}, t_{SND} and t_{DRP} be the mean sojourn time of a CR node in the states BF_i, SND and DRP, respectively. The probabilities that a CR node is at the states BF_i, SND and DRP are

$$
\begin{aligned}
P_{\mathrm{BF}_i} &= \frac{(\pi_{\mathrm{BF}_i})\ t_{\mathrm{BF}_i}}{T_{mac}} \qquad i = 0, ..., K-1 \\
P_{\mathrm{SND}} &= \frac{(\pi_{\mathrm{SND}})\ t_{\mathrm{SND}}}{T_{mac}} \\
P_{\mathrm{DRP}} &= \frac{(\pi_{\mathrm{DRP}})\ t_{\mathrm{DRP}}}{T_{mac}}
\end{aligned}
\tag{25}
$$

where

$$
\begin{aligned}
& T_{mac} = (\pi_{\mathrm{SND}})t_{\mathrm{SND}} + (\pi_{\mathrm{DRP}})t_{\mathrm{DRP}} + \sum_{i=0}^{K-1} (\pi_{\mathrm{BF}_i})t_{\mathrm{BF}_i} \\
& t_{\mathrm{BF}_i} = 2^{i-1} BT_{min} \qquad i = 0, ..., K-1 \\
& t_{\mathrm{SND}} = \frac{8 \times S_{\mathrm{pkt}}}{C} \\
& t_{\mathrm{DRP}} \approx 0
\end{aligned}
\tag{26}
$$

and the S_{pkt} and C are packet size in bytes and channel bandwidth in bits per second, respectively.

Let N_{c} be the number of contending neighbor nodes of a CR node in acquisition of spectrum channels. The backoff probability of a CR node depends on the sending probability of the contending neighbor nodes that can be calculated as:

$$
p_b = 1 - (1 - P_{\mathrm{SND}})^{\frac{N_{\mathrm{c}}}{P_{\mathrm{off}} N_{\mathrm{ch}}}} \tag{27}
$$

where $\frac{N_{\mathrm{c}}}{P_{\mathrm{off}} N_{\mathrm{ch}}}$ represents average number of CR contending nodes that can use the selected channel of a CR node. The back off probability of a CR node, i.e., p_b, can be simply obtained through Eq. 27 and the second equation of Eq. 25.

When a packet arrives at a CR receiver node while there is already an ongoing reception, we say that a collision has occurred. The collision probability is the probability that a receiving packet at a CR node collides with another packet which is sent by another node. The collision probability can be calculated as:

$$
P_{\mathrm{col}} = 1 - \{P(\mathbf{D} - \mathbf{D}' > t_{\mathrm{rx}})\}^{\frac{N_{\mathrm{c}}}{P_{\mathrm{off}} N_{\mathrm{ch}}}} \tag{28}
$$

where $\mathbf{D}$ and $\mathbf{D}'$ are two random variables representing the MAC delay overhead of two contending CR nodes which have been modeled in Section 5.2. The t_{rx} is the required time for reception of a packet that equals to $\frac{8 \times S_{\mathrm{pkt}}}{C}$.

5.5. Congestion probability in the CRSN

Based on the PDFs of input and the attainable sending rates of a CR node in the CRSN, i.e., $f_{\mathbf{RI}_{h,n}}(r)$ and $f_{\mathbf{RS}}(r)$, the queue length distribution of a CR node is obtained through Eq. 6. If the queue length of a CR sensor be equal

Table 1: CRSN configuration and simulation settings

CRSN topology parameters	
Parameter	**Value/type**
Network area	50 × 50 m^2
Nodes number	19
Nodes spatial distribution	$H = 4, N_0 = 6,$ $N_1 = N_2 = N_3 = N_4 = 3$
Physical and MAC layer parameters	
N_{ch}	6
C	60 Kbps
(α, β)	(3,1)
t_s	0.2 sec
f_s	0.833 Hz
BT_{min}	0.01 sec
K	7
Protocols and parameters of network and transport layers	
Routing protocol	Dynamic Source Routing (DSR)
Queue management strategy	Droptail
Transport protocol	Generic rate-based congestion control schemes (rate-based AIMD and AIAD)
S_{pkt}	30 bytes
R_{max}	120 packets/sec
B, l_{max}	100 packets, 90 packets

or greater than l_{max} (queue length threshold), the CR node is detected as the congested node and the sink station sends a congestion notification command to the sources of the congested path in order to decrease their sending rates. The congestion probability of a CR node is obtained as follows:

$$\Omega = \sum_{l=l_{max}}^{B} Q_l \tag{29}$$

where Q_l is the probability that queue length of CR node equals l. The Q_l is calculated through Eq. 6.

The congestion probability of a path is considered as the congestion probability of the most congested node in the path. Sending rate of the collecting CR sensor of a path is adjusted by rate-based congestion control scheme. Therefore, we have different path congestion probabilities Ω_r per all possible sending rates of path source node ($r = 1, \ldots, R_{max}$). According to Section 4 and based on the Ω_r for all $r = 1, \ldots, R_{max}$, sending rate distribution of CR collecting sensors in transport layer is obtained.

6. Analytical Results and Verifications

We verify the proposed models using simulations through CogNS simulation framework [14] which is a simulation framework for cognitive radio networks based on Network Simulator 2 (NS2) [42]. Default simulation settings and CRSN configuration parameters are summarized in Table 1. The CR network area is 50×50 m^2. The network consists of 6 collecting CR sensors and 12 CR relay nodes and a sink station. The CR relay nodes are distributed in 4 hops (3 nodes at each hop). There are 6 wireless channels (N_{ch}) with the same capacity of 60 Kbps. There is one primary user per channel with the entrance rate (β) of 1 and the departure rate (α) of 3. Sensing time (t_s) and sensing frequency (f_s) are 0.2 second and 0.833 Hz, respectively. The minimum backoff time (BT_{min}) equals to 0.01 second and the maximum number of backoff attempts (K) is considered 7. The dynamic source routing (DSR) protocol [43] is used as routing protocol and the queue management in the network layer is done based on droptail strategy. Generic rate-based AIMD and AIAD schemes are considered as transport protocols. The size of packets (S_{pkt}) is 30 bytes that is the most commonly used packet size for scalar data packets in WSNs [18]. The maximum allowable sending rate (R_{max}) of congestion control schemes is 120 packets per second. The queue size of nodes (B) in network layer is 100 packets and the congestion detection threshold (l_{max}) of queue is 90 packets. In Section 6.1, the sending rate distribution of CR collecting sensors is verified for different rate-based congestion control schemes.

Table 2: Different experiments to present the verification of the rate distribution model

Exp. #	Congestion Control Scheme (INC,DEC)	(t_s, f_s)	(α, β)
(I)	AIMD(1,2)	(0.2sec, 0.833Hz)	(3,1)
(II)	AIMD(1,2)	(0.2sec, 0.833Hz)	(1,3)
(III)	AIMD(1,2)	(0.2sec, 2Hz)	(3,1)
(IV)	AIAD(1,10)	(0.2sec, 0.833Hz)	(3,1)
(V)	AIAD(1,10)	(0.2sec, 0.833Hz)	(1,3)
(VI)	AIAD(1,10)	(0.2sec, 2Hz)	(3,1)

6.1. Verification of Rate Distribution Model

To verify the rate distribution model, it is needed to compare the analytical results with the simulation results for different rate adjustment schemes per various CRSN parameters. Table 2 shows different rate-based congestion control schemes and CR-related parameters which are considered to present the verification of the rate distribution model. We consider AIMD rate adjustment with (INC = 1, DEC = 2) in the experiments (I), (II) and (III), and also AIAD rate adjustment with (INC = 1, DEC = 10) in the experiments (IV), (V) and (VI). The values of default parameters, mentioned in Table 1, are considered in experiments (I) and (IV). The PU activity is set to $(\alpha, \beta) = (1, 3)$ in experiments (II) and (V). The sensing frequency is set to 2 hertz in experiments (III) and (VI).

In figures 5 and 6, the probability mass function (PMF) and cumulative mass function (CMF) of the sending rate of CR collecting sensors obtained from the simulations are compared with those obtained from the proposed stochastic models (the Sections 4 and 5). The PMFs of sending rate for the experiments (I), (II), (III), (IV), (V) and (VI) are depicted in figures 5(a), 5(c), 5(e), 6(a), 6(c) and 6(e), respectively. In addition, the figures 5(b), 5(d), 5(f), 6(b), 6(d) and 6(f) illustrate the CMFs of sending rate for the experiments (I), (II), (III), (IV), (V) and (VI), respectively. In all cases, we see the close match between the analytic and simulation results with a small deviation. In figures 5(a), 5(c) and 5(e), the mean rates that are calculated by model are 59.83, 49.23 and 41.85

packets per second and mean rates that are obtained through simulation are 61.30, 50.34 and 42.84 packets per second according to the experiments (I), (II) and (III), respectively. In the figures 6(a), 6(c) and 6(e), the mean rates that are calculated by model are 77.41, 63.44 and 53.28 packets per second and mean rates that are obtained through simulation are 78.74, 62.52 and 54.57 packets per second according to the experiments (IV), (V) and (VI), respectively. It is obvious that when the primary user activity is increased, average rate decreases; also when sensing frequency is increased, the average rate decreases.

7. Conclusions

In this paper, we have modeled MAC-layer delay overhead of a CR node. Based on the MAC-layer delay model, the probability density functions of CR attainable sending rate and the input rates of different CR nodes have been modeled in the CRSN with regard to the sending rate of the collecting CR sensors in the transport layer. Using the probability density function of input rate and the attainable sending rate of a CR node in the CRSN, steady-state queue length distribution of the CR node has been modeled through a semi-Markov chain (SMC). The congestion probability of each CR node in the network has been calculated using the proposed queue length distribution. The steady-state sending rates distribution of CR collecting sensors have been modeled by semi Markov chains for generic AIMD and generic AIAD congestion control schemes. The sending rate distribution model has been verified through various simulation experiments.

Future studies in this research area could include: (1) obtaining a closed-form formula for the mean sending rate of CR collecting sensors; (2) proposing a rate-based congestion control scheme for cognitive radio sensor networks, (3) investigating on the optimality of rate-based congestion control schemes in CRSNs and (4) studying the possible impacts of CR user mobility on the sending rate distribution of source nodes.

8. Appendix

Theorem 1. Let $\mathbf{X}$ be a random variable with density function $f_{\mathbf{X}}(x)$. Then $\mathbf{Y} = a\mathbf{X}$ is a random variable with density function $f_{\mathbf{Y}}(y) = \frac{1}{a} f_{\mathbf{X}}\left(\frac{y}{a}\right)$ [40].

Theorem 2. Let $\mathbf{X}_1$, $\mathbf{X}_2$, ... , $\mathbf{X}_n$ be n independent random variables with density functions $f_{\mathbf{X}_1}(x)$, $f_{\mathbf{X}_2}(x)$, ... , $f_{\mathbf{X}_n}(x)$. Then the sum $\mathbf{Y} = \mathbf{X}_1 + \mathbf{X}_2 + ... + \mathbf{X}_n$ is a random variable with density function $f_{\mathbf{Y}}(y) = f_{\mathbf{X}_1}(x) * f_{\mathbf{X}_2}(x) * ... * f_{\mathbf{X}_{n}(x)}$ where the right-hand side is an n-fold convolution [40].

Theorem 3. Let $\mathbf{X}$ be a random variable with density function $f_{\mathbf{X}}(x)$. Then $\mathbf{Y} = \frac{1}{\mathbf{X}}$ is a random variable with density function $f_{\mathbf{Y}}(y) = \frac{1}{y^2} f_{\mathbf{X}}\left(\frac{1}{y}\right)$ [40].

Theorem 4. Let $\mathbf{X}$ and $\mathbf{Y}$ be two independent random variables with probability density functions $f_{\mathbf{X}}(x)$ and $f_{\mathbf{Y}}(y)$ and cumulative distribution functions

$F_{\mathbf{X}}(x)$ and $F_{\mathbf{Y}}(y)$ respectively. Then $\mathbf{Z} = \min(\mathbf{X}, \mathbf{Y})$ is a random variable with density function $f_{\mathbf{Z}}(z) = f_{\mathbf{X}}(z) + f_{\mathbf{Y}}(z) - f_{\mathbf{X}}(z)F_{\mathbf{Y}}(z) - F_{\mathbf{X}}(z)f_{\mathbf{Y}}(z)$ [40].

Acknowledgment

The authors would like to thank Dr. Jaafar Almasizadeh for his kind help, and to thank Iran Telecommunication Research Center (ITRC) for supporting this research under grant #T/12591/500 (http://www.itrc.ac.ir).

References

[1] I. F. Akyildiz, W.-Y. Lee, M. C. Vuran, S. Mohanty, Next generation/dynamic spectrum access/cognitive radio wireless networks: A survey, Computer Networks 50 (13) (2006) 2127–2159.

[2] J. Mitola, J. Maguire, G.Q., Cognitive radio: making software radios more personal, IEEE Personal Communications 6 (4) (1999) 13–18.

[3] O. Akan, O. Karli, O. Ergul, Cognitive radio sensor networks, IEEE Network 23 (4) (2009) 34–40.

[4] A. O. Bicen, O. B. Akan, Reliability and congestion control in cognitive radio sensor networks, Ad Hoc Networks 9 (7) (2011) 1154–1164.

[5] A. O. Bicen, V. C. Gungor, O. B. Akan, Delay-sensitive and multimedia communication in cognitive radio sensor networks, Ad Hoc Networks 10 (5) (2012) 816–830.

[6] A. Slingerland, P. Pawelczak, R. Venkatesha Prasad, A. Lo, R. Hekmat, Performance of transport control protocol over dynamic spectrum access links, in: 2nd IEEE DySPAN 2007, pp. 486–495.

[7] Y. Kondareddy, P. Agrawal, Effect of dynamic spectrum access on transport control protocol performance, in: IEEE GLOBECOM 2009, pp. 1–6.

[8] M. Di Felice, K. R. Chowdhury, W. Kim, A. Kassler, L. Bononi, End-to-end protocols for cognitive radio ad hoc networks: An evaluation study, Performance Evaluation 68 (9) (2011) 859–875.

[9] K. Chowdhury, M. Di Felice, I. Akyildiz, TP-CRAHN: a transport protocol for cognitive radio ad-hoc networks, in: IEEE INFOCOM 2009, pp. 2482–2490.

[10] D. Sarkar, H. Narayan, Transport layer protocols for cognitive networks, in: IEEE INFOCOM 2010, pp. 1–6.

[11] E. S. Hosseini, V. Esmaeelzadeh, R. Berangi, O. B. Akan, A correlation-based and spectrum-aware admission control mechanism for multimedia streaming in cognitive radio sensor networks, International Journal of Communication Systems, in press,doi:10.1002/dac.2986.

[12] T. Issariyakul, L. Pillutla, V. Krishnamurthy, Tuning radio resource in an overlay cognitive radio network for TCP: greed isn't good, IEEE Communications Magazine 47 (7) (2009) 57–63.

[13] A. K. Al-Ali, K. Chowdhury, TFRC-CR: an equation-based transport protocol for cognitive radio networks, Ad Hoc Networks 11 (6) (2013) 1836–1847.

[14] V. Esmaeelzadeh, R. Berangi, S. M. Sebt, E. S. Hosseini, M. Parsinia, CogNS: a simulation framework for cognitive radio networks, Wireless Personal Communications 72 (4) (2013) 2849–2865.

[15] V. Esmaeelzadeh, R. Berangi, On the optimality of generic rate-based AIMD and AIAD congestion control schemes in cognitive radio sensor networks, International Journal of Distributed Sensor Networks, Article ID 614643, in press.

[16] V. Esmaeelzadeh, R. Berangi, E. S. Hosseini, O. B. Akan, Stochastic backlog and delay bounds of generic rate-based AIMD congestion control scheme in cognitive radio sensor networks, Pervasive and Mobile Computing, in press,doi:10.1016/j.pmcj.2015.02.005.

[17] Y. Jiang, Y. Liu, Stochastic Network Calculus, Springer, London, 2008.

[18] A. J. D. Rathnayaka, V. M. Potdar, Wireless sensor network transport protocol: A critical review, Journal of Network and Computer Applications 36 (1) (2013) 134–146.

[19] M. Kafi, D. Djenouri, J. Ben-Othman, N. Badache, Congestion control protocols in wireless sensor networks: A survey, IEEE Communications Surveys Tutorials 16 (3) (2014) 1369–1390.

[20] O. Akan, I. Akyildiz, Event-to-sink reliable transport in wireless sensor networks, IEEE/ACM Transactions on Networking 13 (5) (2005) 1003–1016.

[21] V. Gungor, O. Akan, I. Akyildiz, A real-time and reliable transport (rt) protocol for wireless sensor and actor networks, IEEE/ACM Transactions on Networking 16 (2) (2008) 359–370.

[22] C.-Y. Wan, S. B. Eisenman, A. T. Campbell, CODA: congestion detection and avoidance in sensor networks, in: 1st International Conference on Embedded Networked Sensor Systems 2003, ACM, New York, USA, pp. 266–279.

[23] B. Hull, K. Jamieson, H. Balakrishnan, Mitigating congestion in wireless sensor networks, in: 2nd International Conference on Embedded Networked Sensor Systems 2004, ACM, New York, USA, pp. 134–147.

[24] C.-Y. Wan, S. B. Eisenman, A. T. Campbell, J. Crowcroft, Siphon: Overload traffic management using multi-radio virtual sinks in sensor networks, in: 3rd International Conference on Embedded Networked Sensor Systems 2005, ACM, New York, USA, pp. 116–129.

[25] Y. Iyer, S. Gandham, S. Venkatesan, STCP: a generic transport layer protocol for wireless sensor networks, in: ICCCN 2005, pp. 449–454.

[26] V. Gungor, O. Akan, DST: delay sensitive transport in wireless sensor networks, in: International Symposium on Computer Networks 2006, pp. 116–122.

[27] E. Giancoli, F. Jabour, A. Pedroza, CTCP: reliable transport control protocol for sensor networks, in: ISSNIP 2008, pp. 493–498.

[28] F. Shaikh, A. Khelil, A. Ali, N. Suri, TRCCIT: tunable reliability with congestion control for information transport in wireless sensor networks, in: Wireless Internet Conference (WICON) 2010, pp. 1–9.

[29] C. Wang, B. Li, K. Sohraby, M. Daneshmand, Y. Hu, Upstream congestion control in wireless sensor networks through cross-layer optimization, IEEE Journal on Selected Areas in Communications 25 (4) (2007) 786–795.

[30] C. Sergiou, V. Vassiliou, Alternative path creation vs data rate reduction for congestion mitigation in wireless sensor networks, in: Proceedings of the 9th ACM/IEEE International Conference on Information Processing in Sensor Networks 2010, pp. 394–395.

[31] J. Paek, R. Govindan, RCRT: rate-controlled reliable transport protocol for wireless sensor networks, ACM Transactions Sensor Networks 7 (3) (2010) 20:1–20:45.

[32] Y. Zhou, M. Lyu, J. Liu, H. Wang, PORT: a price-oriented reliable transport protocol for wireless sensor networks, in: ISSRE 2005, pp. 117–126.

[33] S. Kim, R. Fonseca, P. Dutta, A. Tavakoli, D. Culler, P. Levis, S. Shenker, I. Stoica, Flush: A reliable bulk transport protocol for multihop wireless networks, in: Proceedings of the 5th International Conference on Embedded Networked Sensor Systems 2007, ACM, pp. 351–365.

[34] S. Brahma, M. Chatterjee, K. Kwiat, Congestion control and fairness in wireless sensor networks, in: 8th IEEE International Conference on Pervasive Computing and Communications Workshops (PERCOM Workshops) 2010, pp. 413–418.

[35] I. F. Akyildiz, W. Su, Y. Sankarasubramaniam, E. Cayirci, Wireless sensor networks: A survey, Computer Networks 38 (4) (2002) 393–422.

[36] W.-Y. Lee, I. Akyildiz, Optimal spectrum sensing framework for cognitive radio networks, IEEE Transactions on Wireless Communications 7 (10) (2008) 3845–3857.

[37] B. F. Lo, A survey of common control channel design in cognitive radio networks, Physical Communication 4 (1) (2011) 26–39.

[38] O. B. Akan, On the throughput analysis of rate-based and window-based congestion control schemes, Computer Networks 44 (5) (2004) 701–711.

[39] K. S. Trivedi, Probability and Statistics with Reliability, Queueing, and Computer Science Applications, 2nd Edition, Wiley-Interscience, 2001.

[40] S. Miller, D. Childers, Probability and Random Processes: With Applications to Signal Processing and Communications, 2nd Edition, Academic Press, 2004.

[41] Y. Wang, M. C. Vuran, S. Goddard, Cross-layer analysis of the end-to-end delay distribution in wireless sensor networks, IEEE/ACM Transactions on Networking 20 (1) (2012) 305–318.

[42] Network simulator version 2, `http://www.isi.edu/nsnam/ns/`.

[43] D. Johnson, D. Maltz, Y. Hu, J. Jetcheva, The dynamic source routing protocol for mobile ad hoc networks (DSR), IETF Internet draft, 2002.

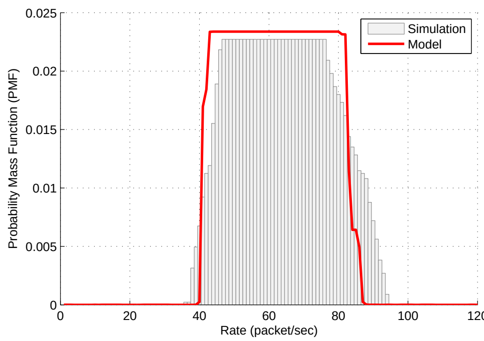

(a) The PMF of sending rate in experiment (I)

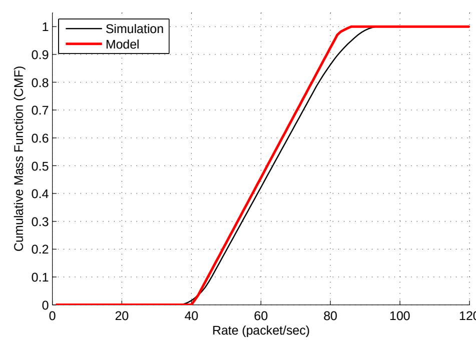

(b) The CMF of sending rate in experiment (I)

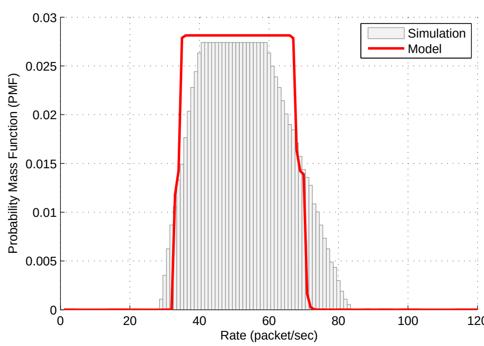

(c) The PMF of sending rate in experiment (II)

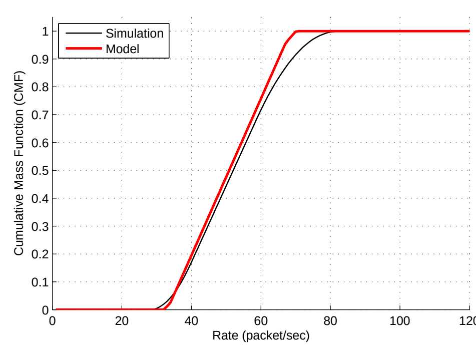

(d) The CMF of sending rate in experiment (II)

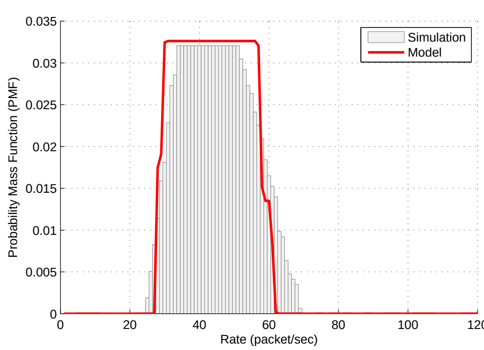

(e) The PMF of sending rate in experiment (III)

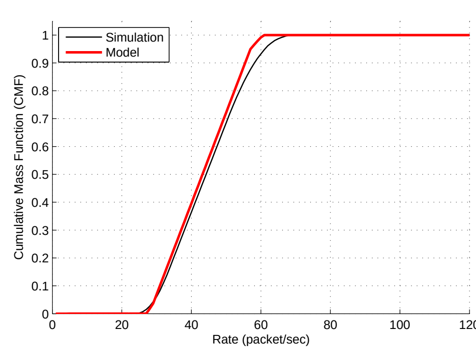

(f) The CMF of sending rate in experiment (III)

Figure 5: Verification of the sending rate distribution of CR collecting sensors in congestion control schemes by the experiments (I), (II) and (III) mentioned in Table 2.

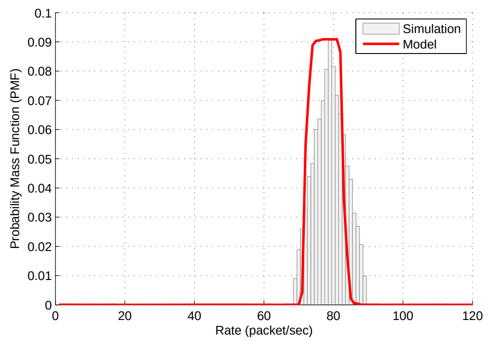

(a) The PMF of sending rate in experiment (IV)

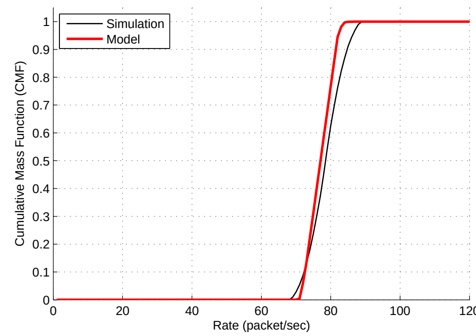

(b) The CMF of sending rate in experiment (IV)

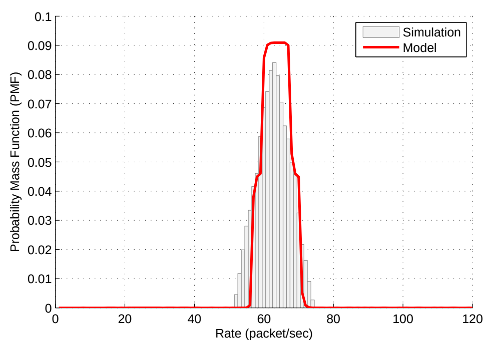

(c) The PMF of sending rate in experiment (V)

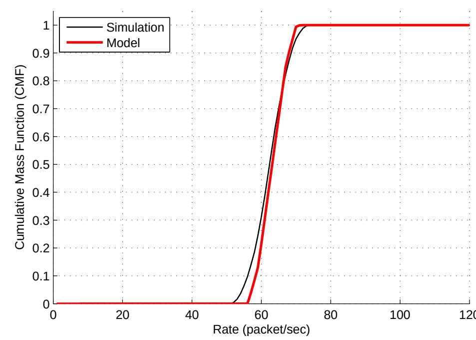

(d) The CMF of sending rate in experiment (V)

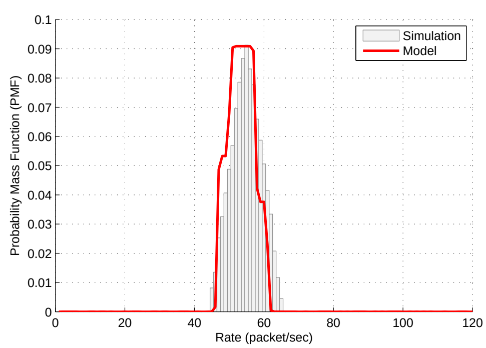

(e) The PMF of sending rate in experiment (VI)

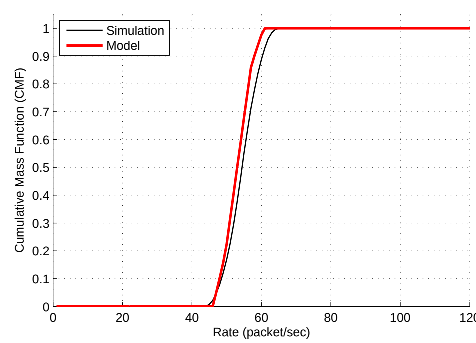

(f) The CMF of sending rate in experiment (VI)

Figure 6: Verification of the sending rate distribution of CR collecting sensors in congestion control schemes by the experiments (IV), (V) and (VI) mentioned in Table 2.